

## Theoretical approach to Rayleigh and absorption spectra of semiconducting carbon nanotubes

Ermin Malić<sup>\*,1,2</sup>, Matthias Hirtschulz<sup>2</sup>, Frank Milde<sup>2</sup>, Yang Wu<sup>3</sup>, Janina Maultzsch<sup>3</sup>, Tony F. Heinz<sup>3</sup>, Andreas Knorr<sup>2</sup>, and Stephanie Reich<sup>1</sup>

<sup>1</sup> Department of Materials Science and Engineering, Massachusetts Institute of Technology, 02139 Cambridge, USA

<sup>2</sup> Institut für Theoretische Physik, Nichtlineare Optik und Quantenelektronik, Technische Universität Berlin, 10623 Berlin, Germany

<sup>3</sup> Departments of Physics and Electrical Engineering, Columbia University, New York 10027, USA

Received 1 May 2007, revised 19 June 2007, accepted 19 June 2007

Published online 26 September 2007

PACS 78.35.+c, 78.67.Ch

A microscopic calculation of the Rayleigh scattering cross section and the absorption coefficient for arbitrary single-walled carbon nanotubes is presented. The approach is based on the density matrix formalism combined with the tight-binding band structure. Both Rayleigh and absorption spectra show a characteristic intensity ratio behavior, which can be explained by an interplay of the optical matrix element and the joint density of states.

© 2007 WILEY-VCH Verlag GmbH & Co. KGaA, Weinheim

### 1 Introduction

Over the recent years Rayleigh scattering from nanoscale objects, such as single-walled carbon nanotubes (SWCNTs) [1, 2] and semiconductor quantum wells [3–5] was successfully added to long-established optical spectroscopy methods, such as absorption, photoluminescence and Raman spectroscopy [6–8]. Combined with electron diffraction data Rayleigh scattering spectroscopy has successfully been applied to determine the physical structure of individual SWCNTs [2]. In contrast to the optical absorption coefficient that is given by the imaginary part of the optical susceptibility [9, 10], the Rayleigh scattering cross section is determined by the full dielectric response of the investigated nanotube [11]. This difference leads to unique features in Rayleigh spectra, which will be discussed in this work.

### 2 Rayleigh scattering cross section and absorption coefficient

Within the approximation that Rayleigh scattering from SWCNTs corresponds to scattering from a cylinder with a diameter small compared to the wavelength of light, we obtain for the Rayleigh scattering cross section per unit length [1, 11]:

$$\sigma(\omega) \propto r^4 \omega^3 |\varepsilon(\omega) - 1|^2, \quad (1)$$

where  $\omega$  is the frequency of the scattered light,  $r$  the radius of the cylinder, and  $\varepsilon(\omega)$  the dielectric function of the nanotube. The frequency dependent optical susceptibility  $\chi(\omega) = \varepsilon(\omega) - 1$  is the response

\* Corresponding author: e-mail: ermin@itp.physik.tu-berlin.de

function of the perturbed system [9]. It contains information about physical structure, electronic transitions, as well as the chirality and family dependence of the individual SWCNT. In contrast to the Rayleigh scattering cross section from Eq. (1), the absorption coefficient  $\alpha(\omega)$  is given only by the imaginary part of the susceptibility  $\chi(\omega)$  [9, 10]:

$$\alpha(\omega) \propto \omega \operatorname{Im} \chi(\omega). \quad (2)$$

To obtain the absorption coefficient  $\alpha$  and the Rayleigh scattering cross section  $\sigma(\omega)$  we have to determine  $\chi(\omega)$  which is defined as a function of the macroscopic current density  $j(\omega)$  and the vector potential  $A(\omega)$  [10, 12]. The current density  $j(t) \propto -i(2e_0\hbar/m_0) \sum_k \operatorname{Re}[M_z(\mathbf{k})p_k(t)]$  depends on the optical

matrix element  $M_z(\mathbf{k})$  along the nanotube axis ( $z$ -axis) and the microscopic polarization  $p_k(t)$ . The latter expresses the probability amplitude for an optical transition at the wave vector  $\mathbf{k}$  and can be calculated within the density matrix formalism by solving the free-particle Bloch equation [9]  $\dot{p}_k(t) = -i\Delta\omega_k p_k(t) + g_k(t) - \gamma p_k(t)$ . The microscopic polarization  $p_k(t)$  is determined by the subband transition frequency  $\Delta\omega_k = [\omega_c(\mathbf{k}) - \omega_v(\mathbf{k})]$  (where  $c$  denotes the conduction band and  $v$  the valence band), the Rabi frequency  $g_k(t) = (e_0/m_0) M_z(\mathbf{k}) A(t)$  (with  $m_0$  as the bare electron mass and  $e_0$  as the elementary charge), and the phenomenological parameter  $\gamma$  introduced to describe dephasing resulting from electron–phonon or electron–photon coupling. As a first approach, we focus on the free-particle Bloch equation. Even though the optical excitations of carbon nanotubes are determined by excitons [13, 14], free-particle band-to-band transitions form a first fundamental step in understanding the optical properties of carbon nanotubes, especially their chirality and family behavior [10, 15, 16]. The calculation of the cross section  $\sigma(\omega)$  from Eq. (1) and the absorption coefficient  $\alpha(\omega)$  from Eq. (2) requires, finally, the determination of the optical matrix element  $M(\mathbf{k})$ . Within the tight-binding model and the orthogonal first-neighbor approximation [17–20], we obtain a fully analytical expression for  $M_z(\mathbf{k})$  for light polarized along the nanotube axis [10]:

$$M_z(m, k_z) = \frac{M_c}{2\sqrt{N}|e(\mathbf{k})|} [(n_1 - n_2) \cos \Psi_3 - (2n_1 + n_2) \cos \Psi_1 + (n_1 + 2n_2) \cos \Psi_2], \quad (3)$$

with the constant optical matrix element  $M_c$  for the two nearest-neighbor atoms [15],  $N = n_1^2 + n_2^2 + n_1 n_2$ ,  $\Psi_1 = \pi m (2n_1 + n_2)/N - 2\pi (n_2/q) k_z$ ,  $\Psi_2 = \pi m (n_1 + 2n_2)/N + 2\pi (n_1/q) k_z$ ,  $\Psi_3 = \Psi_1 - \Psi_2$ , and  $|e(\mathbf{k})| = \sqrt{\sum_{i=1}^3 [1 + 2 \cos(\Psi_i)]}$ . The number of graphene hexagons in the nanotube unit cell is denoted by  $q$  [17].

The matrix element is a function of the chiral index  $(n_1, n_2)$  and of  $\mathbf{k}$ , which contains the band index  $m$  and the wave vector  $k_z$  along the tube axis. It exhibits an important nanotube family dependence as discussed below, see also [10]. Now, we have all ingredients to calculate  $\sigma(\omega)$  and  $\alpha(\omega)$ . The results are presented in the next section.

### 3 Rayleigh and absorption spectra of semiconducting carbon nanotubes

Figure 1 compares absorption and Rayleigh spectra showing the third and fourth transition  $E_{33}$  and  $E_{44}$  in semiconducting carbon nanotubes with an approximately constant diameter of about 2 nm. We focus on these nanotubes, since experimental Rayleigh spectra of SWCNTs with a similar diameter have already been measured [1, 2]. In contrast to the absorption coefficient  $\alpha(\omega)$ , the Rayleigh scattering cross section  $\sigma(\omega)$  also contains the real part of the dielectric function  $\varepsilon(\omega)$  [Eq. (1)]. The latter leads to some unique features in Rayleigh spectra. Figure 1 illustrates that Rayleigh peaks have a different lineshape and are slightly red-shifted compared to the corresponding Van Hove singularities in the absorption spectra. The real part of the dielectric function  $\varepsilon(\omega)$  (refractive index contribution) has a non-resonant tail on the lower energy side of each transition [9] leading to the asymmetric broadening of the Van Hove singularities. The slight difference in the maxima positions of the imaginary and the real part of  $\varepsilon(\omega)$  accounts for

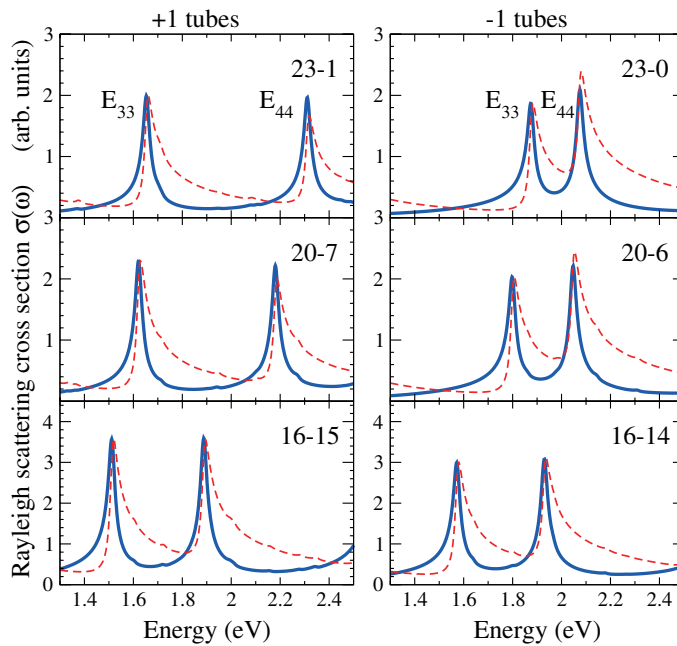


**Fig. 1** (online colour at: [www.pss-b.com](http://www.pss-b.com)) Rayleigh spectra of semiconducting +1 and -1 nanotubes with a diameter of approx. 2 nm corresponding to the Kataura branch [21] with  $2n_1 + n_2 = 48$ . The chiral angle increases from top to bottom. Note that for -1 tubes the energetically lower transition  $E_{33}$  is weaker in intensity, whereas +1 tubes show an inverse behavior. The figure also illustrates the corresponding absorption spectra (dashed line) with the characteristic Van Hove singularities. (The absorption coefficient is normalized to the value of the  $E_{33}$  peak in the corresponding Rayleigh spectra.)

the red-shift of Rayleigh peaks. This shift is about 10 meV, and it is independent of the chiral angle or the nanotube family.

Figure 1, furthermore, shows that for semiconducting -1 tubes, i.e. tubes belonging to the  $(n_1 - n_2) \times \text{mod}3 = -1$  family [17, 21], the third transition  $E_{33}$  is weaker in intensity than  $E_{44}$ . In contrast, the semiconducting +1 tubes belonging to the  $(n_1 - n_2) \text{mod}3 = +1$  family have the opposite behavior:  $E_{33}$  is slightly stronger in intensity. This different family behavior cannot be explained by considering only the joint density of states (JDOS), which has been shown to be generally enhanced for energetically higher transitions [10, 18]. As a result, the transitions  $E_{33}$  is expected to be smaller in intensity than  $E_{44}$  independently of the tube family – in contrast to our observation in Fig. 1. An explanation can be found when taking the optical matrix element  $M_z(\mathbf{k})$  into account. Figure 2 shows  $M_z(\mathbf{k})$  along the  $\Gamma KM$  high-symmetry line of graphene. The matrix element has a smaller absolute value on the  $\Gamma K$ - than on the  $KM$ -side. This leads to a family dependence of  $M_z(\mathbf{k})$ , which has an influence on the oscillator strength of

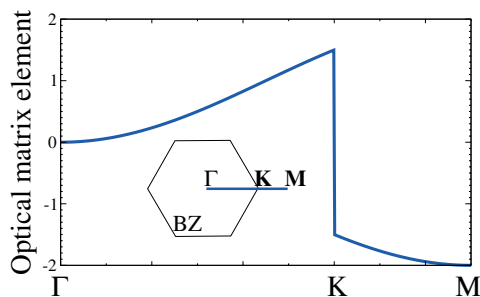


**Fig. 2** (online colour at: [www.pss-b.com](http://www.pss-b.com)) Optical matrix element  $M_z(\mathbf{k})$  at the  $\Gamma$  point of a zigzag nanotube ( $k_z = 0$ ), at which the subband transitions take place. This plot corresponds to the  $\Gamma KM$  high-symmetry line of graphene. The inset shows the Brillouin zone of graphene with the line  $\Gamma KM$ . Note, that the matrix element  $M_z(m, 0)$  has a smaller absolute value on the  $\Gamma K$ - than on the  $KM$ -side. This has an influence on the oscillator strength of transitions.

transitions. Depending on the side, on which the Van Hove singularity is located with respect to the  $K$  point, the transition intensity is expected to be enhanced or reduced. The observed different family behavior of relative intensities in Fig. 1 arises from the fact that the energy minima for +1 and -1 tubes for a given transition  $E_{ii}$  are located on opposite sides of the graphene  $K$  point [10, 21]. For +1 tubes the  $E_{33}$  Van-Hove singularity originates from the  $KM$ -line (whereas  $E_{44}$  stems from the  $TK$ -line) [10, 21] resulting in an enhancement of  $E_{33}$  with respect to  $E_{44}$ , since the matrix element  $M_z(\mathbf{k})$  is larger on the  $KM$ -side (Fig. 2). The difference in intensity for +1 tubes, however, is much smaller than for -1 tubes, see Fig. 1. This can be led back to the geometry factor  $\omega^3 r^4$  in Eq. (1) that enhances the energetically higher transition  $E_{44}$  leading to a reduction of the intensity differences for +1 tubes.

## 4 Conclusions

In conclusion, we have calculated the Rayleigh scattering cross section and the absorption coefficient for arbitrary carbon nanotubes within the density matrix formalism and the tight-binding model. We show that Rayleigh peaks have a different lineshape and are slightly red-shifted compared to the corresponding Van Hove singularities in the absorption spectra. Furthermore, the chirality and family dependence of the characteristic intensity ratios in both Rayleigh and absorption spectra is explained by an interplay of the joint density of states and the optical matrix elements. Our work will be useful for the optical characterization of semiconducting single-walled carbon nanotubes.

**Acknowledgements** We thank C. Thomsen (TU Berlin) for valuable discussions. E.M. is grateful to *Studienstiftung des deutschen Volkes* for financial support. J.M. acknowledges support from the *Alexander-von-Humboldt foundation*.

## References

- [1] M. Y. Sfeir et al., *Science* **306**, 1540 (2004).
- [2] M. Y. Sfeir et al., *Science* **312**, 554 (2006).
- [3] G. Kocherscheidt et al., *Phys. Rev. B* **68**, 085207 (2003).
- [4] A. Thränhardt et al., *Phys. Rev. B* **62**, 16802 (2000).
- [5] A. Thränhardt et al., *Phys. Rev. B* **62**, 2706 (2000).
- [6] S. M. Bachilo et al., *Science* **298**, 2361 (2002).
- [7] Y. Miyauchi et al., *Chem. Phys. Lett.* **387**, 198 (2004).
- [8] H. Telg et al., *Phys. Rev. Lett.* **93**, 177401 (2004).
- [9] H. Haug and S. W. Koch, *Quantum Theory of the Optical and Electronic Properties of Semiconductors* (World Scientific, Singapore, 2004).
- [10] E. Malić et al., *Phys. Rev. B* **74**, 195431 (2006).
- [11] C. F. Bohren and D. R. Huffman, *Absorption and Scattering of Light by Small Particles* (Wiley-VCH, Weinheim, 2004).
- [12] M. Kira, W. Hoyer, and S. W. Koch, *phys. stat. sol. (b)* **238**, 443 (2003).
- [13] F. Wang, G. Dukovic, L. E. Brus, and T. F. Heinz, *Science* **308**, 838 (2005).
- [14] J. Maultzsch et al., *Phys. Rev. B* **72**, 241402(R) (2005).
- [15] A. Grüneis et al., *Phys. Rev. B* **67**, 165402 (2003).
- [16] S. V. Goupalov, *Phys. Rev. B* **72**, 195403 (2005).
- [17] S. Reich, C. Thomsen, and J. Maultzsch, *Carbon Nanotubes: Basic Concepts and Physical Properties* (Wiley-VCH, Berlin, 2004).
- [18] R. Saito, G. Dresselhaus, and M. S. Dresselhaus, *Phys. Rev. B* **61**, 2981 (2000).
- [19] S. Reich, J. Maultzsch, C. Thomsen, and P. Ordejón, *Phys. Rev. B* **66**, 035412 (2002).
- [20] V. N. Popov and L. Henrard, *Phys. Rev. B* **70**, 115407 (2004).
- [21] C. Thomsen and S. Reich, *Raman Scattering in Carbon Nanotubes*, in: *Light Scattering in Solids IX*, edited by M. Cardona and R. Merlin (Springer, Berlin, 2007).